



Synergistic anticancer activities of the plant-derived sesquiterpene lactones salograviolide A and iso-seco-tanaparholide

Mohamed Salla · Isabelle Fakhoury ·
Najat Saliba · Nadine Darwiche · Hala Gali-Muhtasib

Received: 6 April 2012 / Accepted: 8 August 2012 / Published online: 14 September 2012
© The Japanese Society of Pharmacognosy and Springer 2012

Abstract We have previously shown that the two sesquiterpene lactones, salograviolide A (Sal A) and iso-seco-tanaparholide (TNP), isolated from the Middle Eastern indigenous plants *Centaurea ainetensis* and *Achillea falcata*, respectively, possess selective antitumor properties. Here, we aimed to assess the anticancer effects of the separate compounds and their combination, study their potential to generate reactive oxygen species (ROS), and investigate their underlying antitumor mechanisms in human colon cancer cell lines. Cells were treated with Sal A and TNP alone or in combination, and cell viability, cell cycle profile, apoptosis, ROS generation and changes in protein expression were monitored. Sal A and TNP in combination caused

80 % decrease in HCT-116 and DLD-1 cell viability versus only 25 % reduction when the drugs were used separately. The antitumor mechanism involved triggering ROS-dependent apoptosis as well as disruption of the mitochondrial membrane potential. Further studies showed that apoptosis by the Sal A and TNP combination was caspase-independent and that ERK, JNK and p38 of the serine/threonine MAPKs signaling pathway were involved in the cell death mechanism. Taken together, our data suggest that the combination of Sal A and TNP may be of therapeutic interest against colon cancer.

Keywords Anticancer · Colon cancer · Sesquiterpene lactones · Reactive oxygen species · Combination therapy · Synergism

M. Salla and I. Fakhoury contributed equally

M. Salla · I. Fakhoury · H. Gali-Muhtasib (✉)
Department of Biology, American University of Beirut,
Riad El-Solh, Beirut, Lebanon
e-mail: amro@aub.edu.lb

M. Salla
e-mail: mohammad.sallah@liu.edu.lb

I. Fakhoury
e-mail: ihf04@aub.edu.lb

N. Saliba
Department of Chemistry, American University of Beirut,
Riad El-Solh, Beirut, Lebanon
e-mail: ns30@aub.edu.lb

N. Saliba · N. Darwiche · H. Gali-Muhtasib
Ibsar-Nature Conservation Center for Sustainable Futures,
American University of Beirut, Riad El-Solh, Beirut, Lebanon

N. Darwiche
Department of Biochemistry and Molecular Genetics,
American University of Beirut, Riad El-Solh, Beirut, Lebanon
e-mail: nd03@aub.edu.lb

Abbreviations

Bax	Bcl-2-associated X protein
Bcl-2	B cell lymphoma 2
DTT	Dithiothreitol
ERK	Extracellular signal-related kinase
JNK	c-Jun-NH ₂ -terminal kinase
MAPK	Mitogen activated protein kinase
NAC	<i>N</i> -Acetyl cysteine
NF- κ B	Nuclear factor-kappaB
PI	Propidium iodide
ROS	Reactive oxygen species
SL	Sesquiterpene lactone

Introduction

In many cultures, plant extracts have been used to treat various diseases and physical ailments [1]. Secondary metabolites synthesized by plants have been shown to

mediate most of the biological activities of traditionally used plant extracts [2].

Plant secondary metabolites are divided into four major classes, amongst which are the terpenoids [3]. Sesquiterpene lactones (SLs), a subfamily of the terpenoids, comprise thousands of generally colorless bitter phytochemicals of lipophilic nature [4]. Many SLs have shown promising therapeutic potential against cancer when used alone or in combination [4–8]. To date, three SLs have reached cancer clinical trials [reviewed in 4]. Reactive oxygen species (ROS) have been reported to mediate the antitumor activities of SLs [9].

Researchers at the American University of Beirut Nature Conservation Center for Sustainable Futures (Ibsar) have isolated several hydroxylated SLs from Middle Eastern indigenous plants, including is salograviolide A (Sal A) from *Centaurea ainetensis* [10] and iso-seco-tanaparholide (TNP) from *Achillea falcata* [11].

Sal A, which was first isolated in 1992 [12], possesses antifungal [13], antibacterial [14], anti-inflammatory [15], and anti-neoplastic properties [16, 17]. What makes Sal A interesting is its lack of toxicity to normal primary murine keratinocytes and normal human intestinal cells, and its selective inhibition of the growth of neoplastic epidermal benign tumors, squamous cell carcinomas and colon cancer cell lines [16, 17]. We showed that the mechanism underlying Sal A antitumor activity is ROS accumulation, increase in the Pre-G₁ phase of the cell cycle, and apoptosis induction, alongside its ability to modulate key cell cycle regulators and the nuclear factor-kappaB (NF- κ B) signaling pathway [16, 17]. On the other hand, TNP was only tested against the immortalized human keratinocyte cell line HaCat and was found to significantly reduce cell viability [11]. The 3 β -methoxy-iso-seco-tanaparholide isomer of TNP was shown to inhibit promoter-induced cell proliferation of keratinocytes and reduce the proliferation of papilloma and malignant epidermal cells through the modulation of AP-1 and NF- κ B transcriptional activities as well as their downstream targets (N. Darwiche, unpublished results).

Research on the anticancer effects of drug combinations has significantly increased over the past few years. Studies have shown that the combination of several SLs enhances their anticancer, antimicrobial and anti-inflammatory activities [4, 9, 18]. Moreover, the loss of biological activity upon fractionation and purification of plant extracts rich in SLs has suggested a potential synergistic interaction between the different SLs [18]. Regardless of the nature of the combined compounds, drug synergism remains today a phenomenon with great pharmaceutical potential.

The combination of the two plant-derived SLs, Sal A and TNP, has never been investigated against cancer. Therefore, we aimed to assess the effects of these two SLs against

human colon cancer cell lines and investigate their putative oxidative potential and underlying antitumor mechanisms.

Materials and methods

Cell culture

HT-29, HCT-116 and DLD-1 human colon cancer cell lines were cultured in RPMI 1640 with 25 mM HEPES and L-glutamine purchased from Gibco BRL Life Technologies (MA, USA). Normal human intestinal epithelial cells (FHs 74 Int) were cultured in Hybricare medium (ATCC, VA, USA) supplemented with 30 ng/mL of EGF (Biosource, CA, USA), while the normal mouse intestinal Mode-K cells were cultured in DMEM low glucose media supplemented with 2 mM sodium pyruvate (Sigma, MO, USA) and 0.1 mM of non-essential amino acids (Gibco). All media were supplemented with 1 % penicillin/streptomycin (100 U/mL) and 10 % heat-inactivated FBS (Gibco) and cells were grown at 37 °C in a humidified atmosphere of 5 % CO₂ and 95 % air.

Drug preparation and cell treatment

Sal A and TNP (Fig. 1) were extracted and purified from *C. ainetensis* and *A. falcata*, respectively, as described elsewhere [10, 11]. The purity of the compounds was confirmed using hydrogen nuclear magnetic resonance spectroscopy (H-NMR) and gas chromatography coupled with mass spectrometry (GC-MS). Predominant peaks characteristic of each molecule are identified and peaks related to interferences are reduced to a minimum.

The pure compounds, Sal A and TNP, were dissolved in ethanol at concentrations of 27.7 and 35.2 mg/mL. Concentrations ranging between 3 and 20 μ g/mL were obtained by dilution in the cells' respective media. Unless otherwise specified, all cells were seeded at a density of 1×10^5 cells/mL and 24 h later, at 50 % confluency, treated with the desired concentrations for 0.5, 1, 2, 4, 8 or 24 h as indicated. The final ethanol concentration on the cells was less than 0.1 %.

Cytotoxicity and viability assays

Cells were plated in 96-well plates and treated in triplicate with the different concentrations. In some experiments, 5 mM of the antioxidants *N*-acetyl cysteine (NAC) or vitamin C (Sigma) were added to the medium 2 h prior to treatment, while in others, 20 μ M of the pharmacological inhibitors MEK-1 (PD98059) (Cell Signaling Technology, Beverly, MA, USA), p38 (SB203580) (Biosource), JNK (SP600125) (Selleck Chemicals, Houston, TX, USA) or

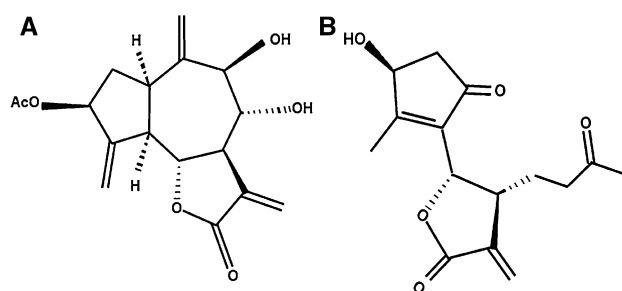


Fig. 1 The chemical structures of Sal A and TNP. **a** Salograviolide A (3 β -acetoxy-8 α ,9 β -dihydroxy-1 α H,5 α H,6 β H,7 α H-guaian-4(15),10(14),11(13)-trien-6,12-olide) with molecular formula C₁₇H₂₀O₆ (320 g/mol). **b** Iso-seco-tanapartholide [(4S,5S)-5-[(3S)-3-hydroxy-2-methyl-5-oxocyclopenten-1-yl]-3-methylidene-4-(3-oxobutyl)oxolan-2-one] with molecular formula C₁₅H₁₈O₅ (278 g/mol)

caspase-9 (Z-LEHD-fmk) (Calbiochem, CA, USA) were added 1 h prior to treatment. Cytotoxicity measured by lactate dehydrogenase release was recorded 6 h post-treatment at 492 nm using the Cell Titer 96 non-radioactive cytotoxicity kit, while viability, as measured by the ability of cells to metabolize tetrazolium salt (MTT), was recorded 24 h after treatment at 570 nm using the Cell Titer 96 non-radioactive cell proliferation assay kit according to the manufacturer's instructions. Both kits were purchased from Promega Corp (WI, USA). The combination indices (CI) and normalized isobolograms were obtained using the CalcuSyn software from Biosoft (Cambridge, MA, UK). The CI formula is: $CI = D_a/D_{ax} + D_b/D_{bx}$, where D indicates the doses of combined Sal A (D_a) and TNP (D_b) inhibiting x % of the cells viability and D_{ax} and D_{bx} indicate the doses of Sal A and TNP alone, respectively, inhibiting x % of the cells viability, as calculated from the equation: $Dx = Dm[fa/(1 - fa)]/m$, where Dm is the median-effect dose of the drug (determined from the x -intercept of the median-effect plot), fa is the fraction affected by the dose, and m is the slope of the median-effect plot.

Cell cycle analysis

Detached cells in the supernatants in addition to the attached cells were collected 24 h after treatment. The pellets were washed with phosphate-buffered saline (PBS) (Gibco), fixed with 70 % ice-cold ethanol and stored at -20 °C overnight. Cells were then washed twice with PBS and incubated with 200 μ g/mL RNase A (Sigma) for 1.5 h at 37 °C before staining with 0.625 μ g/mL of propidium iodide (PI) (Molecular Probes, OR, USA) for 30 min. The fluorescence intensity was measured by flow cytometry using a Fluorescence Activated Cell Sorter (FACS) flow cytometer (Becton–Dickinson, Research Triangle Park,

NC, USA). Cell cycle analysis was performed using the Cell Quest program.

TUNEL assay

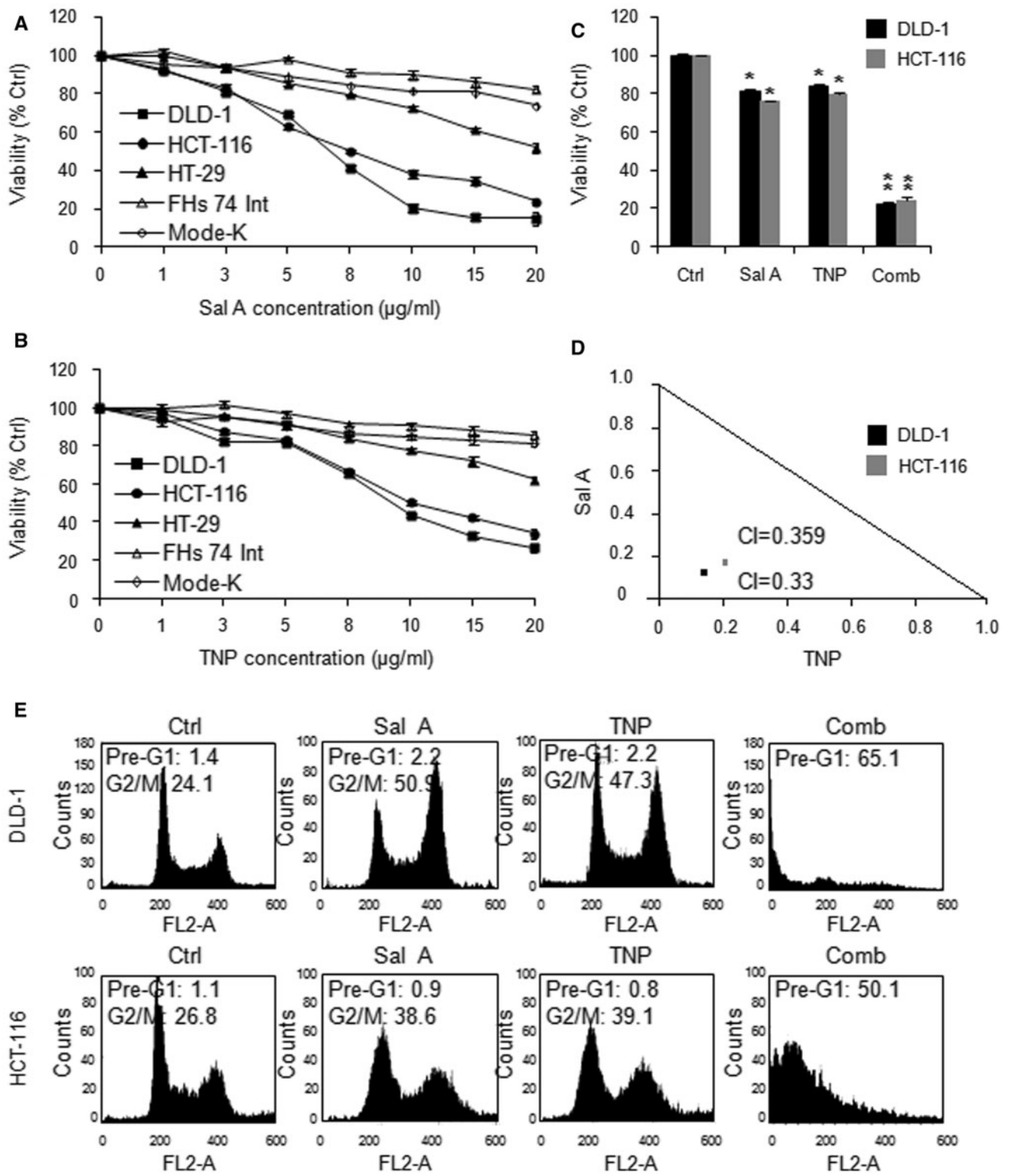
Fragmented DNA was quantified by the terminal deoxytransferase-mediated dUTP nick-end labeling assay (TUNEL). Detached and attached cells were collected 24 h post-treatment, washed twice with PBS, resuspended in 4 % formaldehyde and incubated at room temperature for 30 min. Cells were then pelleted, washed with PBS, resuspended in 100 μ L solution containing PBS, 0.1 % sodium citrate, and 0.1 % Triton X-100 and incubated for 2 min on ice. A second wash of the cells with PBS was followed by suspension in 50 μ L TUNEL reaction mixture consisting of 45 μ L of the labeling solution and 5 μ L of the enzyme solution. After 1 h incubation in the dark in a humidified atmosphere at 37 °C, the mixture was washed and the suspension with 450 μ L of PBS was used for flow cytometry analysis.

DCFH assay

Generation of intracellular H₂O₂ was measured using 5-(and-6)-chloromethyl-2',7'-dichlorodihydrofluorescein diacetate, acetyl ester (CM-H2DCFDA) kit (Invitrogen Molecular Probes, Eugene, OR, USA), a derivative of the DCFDA but with an additional thiol reactive chloromethyl group that enhances the ability of the compound to bind to intracellular components. CM-H2DCFDA is non-fluorescent until removal of the acetate groups by intracellular esterases and oxidation by H₂O₂ to form the highly fluorescent derivative 2'-7'-dichlorofluorescein (DCF). At 50 % confluency, the growth medium (10 % FBS) was replaced by low serum (2 % FBS) media. The cells were treated with the respective drug concentrations (also prepared in low serum media) for 30 min. The medium was subsequently removed and the cells were washed twice and resuspended in 500 μ L of PBS, after which CM-H2DCFDA (10 μ M) was immediately added, and samples were analyzed with a FACS scan flow cytometer on the FL-1 channel with excitation set at 488 nm and emission at 530 nm.

Rhodamine staining

The mitochondrial membrane potential was measured using rhodamine 123 (Invitrogen), a green fluorescent dye that accumulates in active mitochondria with high membrane potential. The cells were plated at a density of 2×10^5 cells/mL and 24 h later treated with the drugs for 6 h before harvesting. The pellets were washed twice in



rhodamine buffer and stained for 30 min at 37 °C by adding 5 µM rhodamine 123 dye. Finally, the cells were washed and resuspended in the rhodamine buffer before reading by flow cytometry.

Protein extraction and Western blotting

The p-ERK (E-4), p-JNK (G-7) and p-p38 (D-8) antibodies and the antimouse and antirabbit IgG-HRP were obtained

Fig. 2 Sal A and TNP combination enhances their growth-suppressive effects in colon cancer cell lines. Normal intestinal cells (FHs 74 Int and Mode-K) and colon cancer cells (HCT-116, DLD-1 and HT-29) were plated in triplicate in 96-well plates at a density of 1×10^5 cells/mL. At 50 % confluency, all cells were treated for 24 h with different concentrations (1–20 $\mu\text{g/mL}$) of Sal A (a) and TNP (b). DLD-1 and HCT-116 were treated with Sal A (3 $\mu\text{g/mL}$), TNP (5 $\mu\text{g/mL}$) and their combination (Comb) (3 $\mu\text{g/mL}$ Sal A with 5 $\mu\text{g/mL}$ TNP) (c). Cell viability (expressed as percentage of control non-treated cells) was determined at 24 h after treatment using the Cell Titer 96 non-radioactive cell proliferation kit as described in “Materials and methods”. HCT-116 and DLD-1 were plated in 6-well plates at a density of 1×10^5 cells/mL. At 50 % confluency, they were treated with Sal A (3 $\mu\text{g/mL}$), TNP (5 $\mu\text{g/mL}$) and their combination (3 $\mu\text{g/mL}$ Sal A with 5 $\mu\text{g/mL}$ TNP). Overlaid normalized isobolograms showing the combination indices (CI) for Sal A (3 $\mu\text{g/mL}$) and TNP (5 $\mu\text{g/mL}$) at 24 h after combination treatment of DLD-1 and HCT-116 cells (d). The CI and normalized isobolograms were obtained using CalcuSyn software with $\text{CI} < 1$ suggesting synergism between Sal A and TNP in both HCT-116 and DLD-1 cell lines. Cell cycle distribution of treated HCT-116 and DLD-1 in Pre- G_1 , S and G_2/M was analyzed by flow cytometry of PI-stained DNA 24 h after treatment (e). The FL2-A signal recorded corresponds to the emitted fluorescent light of the DNA dye FL2 measured as pulse area of the samples. Representative histograms from one of the two separate experiments are shown; each value represents the mean of two independent experiments each done in triplicate. Statistical significance: $*P < 0.05$ and $**P < 0.01$ with respect to control using Dunnett’s multiple comparison test

from Santa Cruz (CA, USA). Bax and Bcl-2 antibodies were from Biosource and the GAPDH was from Biogenesis (Poole, UK). Briefly, cells were seeded in 100 mm dishes, treated with the corresponding concentrations and collected at different time intervals after treatment. Cells were lysed and protein concentrations were determined using the DC BioRad protein assay kit (CA, USA) according to the manufacturer’s instructions. The proteins were then resolved by SDS-PAGE on a 12 % denaturing polyacrylamide gel and transferred onto a PVDF membrane at 30 V overnight. The membrane was immunoblotted with the appropriate primary and secondary antibodies, reacted with enhanced chemiluminescence reagent and exposed to X-ray films for different time periods.

Results

The combination of Sal A and TNP enhances their antitumor activity

Three human colon cancer cell lines (HCT-116, DLD-1 and HT-29) and two normal intestinal cell lines (FHs 74 Int and Mode-K) were treated for 24 h with Sal A or TNP at concentrations ranging between 1 and 20 $\mu\text{g/mL}$. At these concentrations, both compounds are non-cytotoxic to the aforementioned normal cells (data not shown). Figure 2a, b shows no significant reduction of the viability of normal cells in response to increasing concentrations of Sal A or

TNP for up to 15 $\mu\text{g/mL}$. In contrast, both drugs inhibited the viability of all colon cancer cells in a dose-dependent manner, with DLD-1 having the highest sensitivity. The IC_{50} value of Sal A against DLD-1 and HCT-116 was around 8 $\mu\text{g/mL}$ and that of TNP was around 10 $\mu\text{g/mL}$. The same trend was found with Trypan Blue assay (data not shown). These results highlight an important aspect of Sal A and TNP, which is their tumor specificity that enables them to differentially target cancer cells.

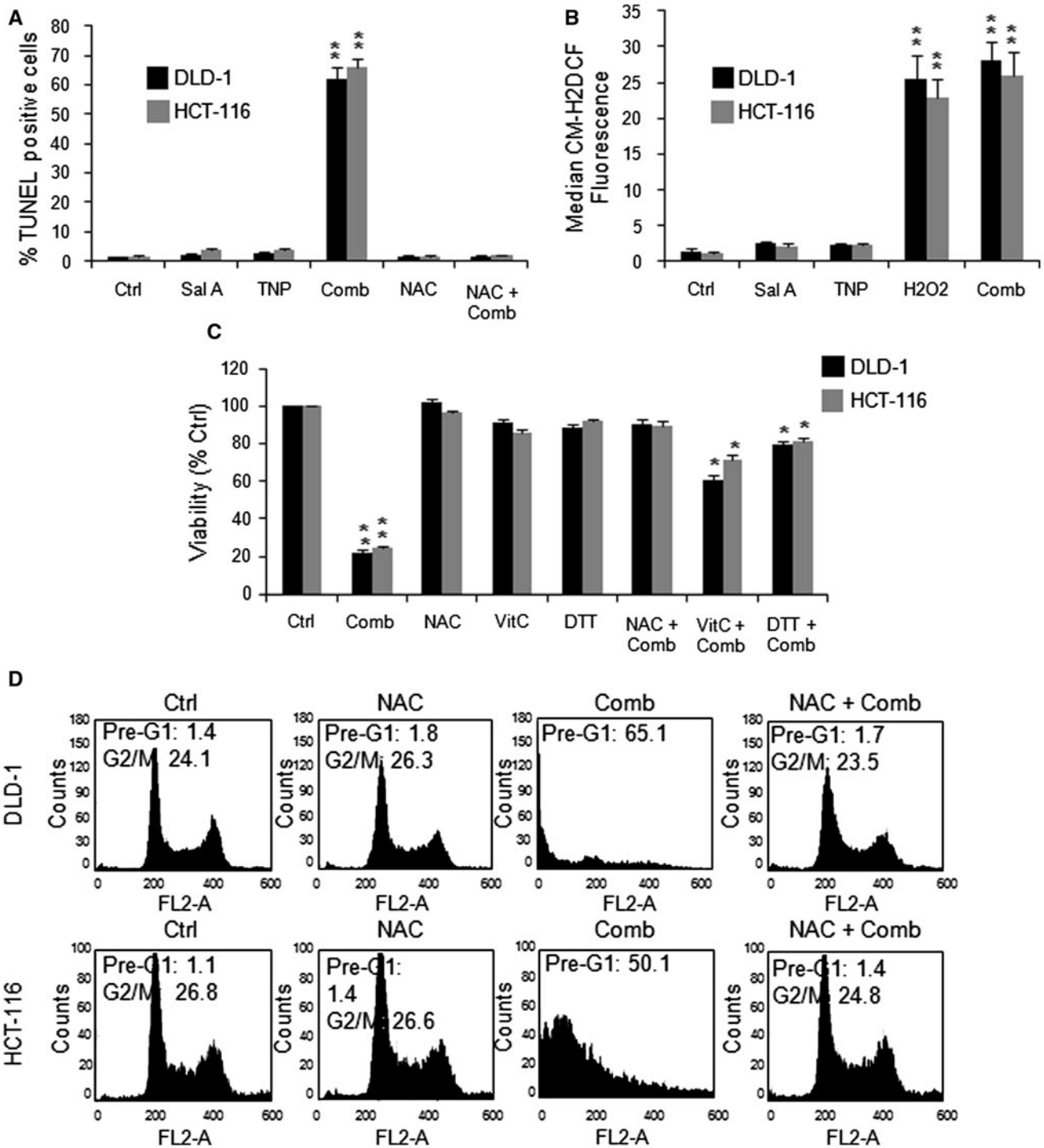
We next aimed at assessing the effect of the drug combination against DLD-1 and HCT-116 cells, as they were the most sensitive to the treatment. We combined different concentrations of Sal A and TNP and found a clear enhancement of the anticancer potential when the cells were subjected to the drug combination compared to the separate treatments. As indicated, Sal A (3 $\mu\text{g/mL}$) and TNP (5 $\mu\text{g/mL}$) alone decreased the viability of both DLD-1 and HCT-116 cells by approximately 20 % whereas the combination treatment caused an 80 % decrease of viability in both cell lines (Fig. 2c). In order to confirm that this outcome is greater than the additive effects of each drug alone, we assessed for drug synergism by the Sal A (3 $\mu\text{g/mL}$) and TNP (5 $\mu\text{g/mL}$) combination in both cell lines using the CalcuSyn software. As shown in the overlaid normalized isobolograms (Fig. 2d), the combination index values (CI) which measure the degree of drug interaction were < 1 , indicating drug synergism.

Cell cycle changes in response to the different treatments were subsequently investigated. As shown in Fig. 2e, the separate treatments with Sal A (3 $\mu\text{g/mL}$) and TNP (5 $\mu\text{g/mL}$) caused a 50 % increase of DLD-1 cells in G_2/M while separate treatments of HCT-116 cells caused 39 and 46 % increases of cells in G_2/M , respectively. The combination treatment, however, induced massive cell death as evidenced by the Pre- G_1 accumulation of 65 % of treated DLD-1 and 50 % of treated HCT-116 cells. Clearly, the combination treatment synergistically enhanced the anticancer potential of the individual compounds.

ROS generation following the combination treatment leads to apoptosis

To determine whether the Pre- G_1 accumulation of treated DLD-1 and HCT-116 cells is due to apoptosis, we performed TUNEL assays. Separate SLs treatments caused less than 5 % of TUNEL-positive DLD-1 and HCT-116 cells, while the combination treatment caused at least 60 % TUNEL positivity (Fig. 3a).

Interestingly, the apoptotic response was completely eliminated after pre-treatment of the cells for 2 h with 5 mM of the strong antioxidant NAC. This suggests an involvement of ROS in the mechanism of cell death induced by the combination treatment. We investigated the



oxidative potential of the drugs using the DCFH assay. Cells were treated with Sal A, TNP or their combination and comparisons were made to control cells or 500 μ M H₂O₂-treated cells. As shown in Fig. 3b, Sal A and TNP alone did not cause significant ROS production in any of the cell lines, whereas the combination resulted in a major oxidative stress. Compared to the control, the combination treatment increased the intracellular levels of ROS by

about 25 times in both cell lines. This pro-oxidant shift was comparable to that induced by 500 μ M H₂O₂, pointing out the important oxidative potential of the combination treatment in targeting colon cancers.

To further assess the role of ROS in cell death, we measured the viability of DLD-1 and HCT-116 cells and analyzed their cell cycle profiles in the presence of the antioxidants NAC, dithiothreitol (DTT), vitamin C and

Fig. 3 Sal A and TNP combination treatment induces ROS and apoptosis in colon cancer cells. The induction of apoptosis in HCT-116 and DLD-1 cells 24 h after treatment with Sal A (3 $\mu\text{g}/\text{mL}$), TNP (5 $\mu\text{g}/\text{mL}$), the combination (3 $\mu\text{g}/\text{mL}$ Sal A with 5 $\mu\text{g}/\text{mL}$ TNP) or pre-treatment with NAC (5 mM for 2 h) followed by the combination was assayed using TUNEL as described in “Materials and methods”. Percent TUNEL positive cells was determined using Cell Quest (a). ROS levels in response to treatment for 30 min with Sal A (3 $\mu\text{g}/\text{mL}$), TNP (5 $\mu\text{g}/\text{mL}$) or the combination (3 $\mu\text{g}/\text{mL}$ Sal A with 5 $\mu\text{g}/\text{mL}$ TNP), or 5 min with 500 μM H_2O_2 were determined by DCFH assay and were expressed as percentage increase over the untreated control (b). DLD-1 and HCT-116 cells were kept at low serum (2 % FBS) at the time of treatment and 10 μM of dye were used. The results represent the median fluorescence of 10,000 counts of each condition. The antioxidants NAC, vitamin C (Vit C) and DTT were all applied at 5 mM for 2 h and followed or not with the combination treatment as indicated. The effect of antioxidant pre-treatment on cell viability was assessed at 24 h (c) and the effect of the NAC antioxidant on cell cycle changes after 24 h of treatment was further assessed (d). Representative histograms from one of the two separate experiments are shown; each value represents the mean of two independent experiments each in triplicate. Statistical significance: * $P < 0.05$ and ** $P < 0.01$ with respect to control using Dunnett’s multiple comparison test. DLD-1 and HCT-116 cells were kept at low serum (2 % FBS) at the time of treatment and 10 μM of dye were used. The results represent the median fluorescence of 10000 counts of each condition. The anti-oxidants NAC, vitamin C (Vit C) and DTT were all applied at 5 mM for 2 h and followed or not with the combination treatment as indicated. The effect of antioxidants pre-treatment on cell viability was assessed at 24 h (c) and the effect of the NAC antioxidant on cell cycle changes after 24 h of treatment was further assessed (d). Representative histograms from one of the two separate experiments are shown; each value represents the mean of two independent experiments each in triplicates. Statistical significance: * $P < 0.05$ and ** $P < 0.01$ with respect to the control using Dunnett’s multiple comparison test

SLs. Pre-treatment of the cells with NAC reversed the combination-induced inhibition in cell viability from 80 to 8 % in DLD-1 cells and from 80 to 13 % in HCT-116 cells (Fig. 3c). Vitamin C and DTT also reversed the inhibition in cell viability but to a lesser extent than NAC. The combination of Sal A and TNP caused 65 % death in DLD-1 cells and 50 % in HCT-116 cells; however, NAC pre-treatment eliminated the accumulation of DLD-1 and HCT-116 cells in Pre- G_1 phase and resulted in a similar cell cycle distribution to control cells (Fig. 3d), which confirms the implication of ROS in cell death.

Mitochondrial membrane permeabilization and MAPKs activation mediate cell death

The mitochondrion is the major site for ROS generation. High ROS production is generally considered a sign of mitochondrial dysfunction [19]. In an attempt to decipher the mechanisms implicated in cell death, we tested the effect of Sal A and TNP combination on the mitochondrial membrane potential using rhodamine 123. As shown in Fig. 4a, Sal A and TNP treatment alone had no effect on

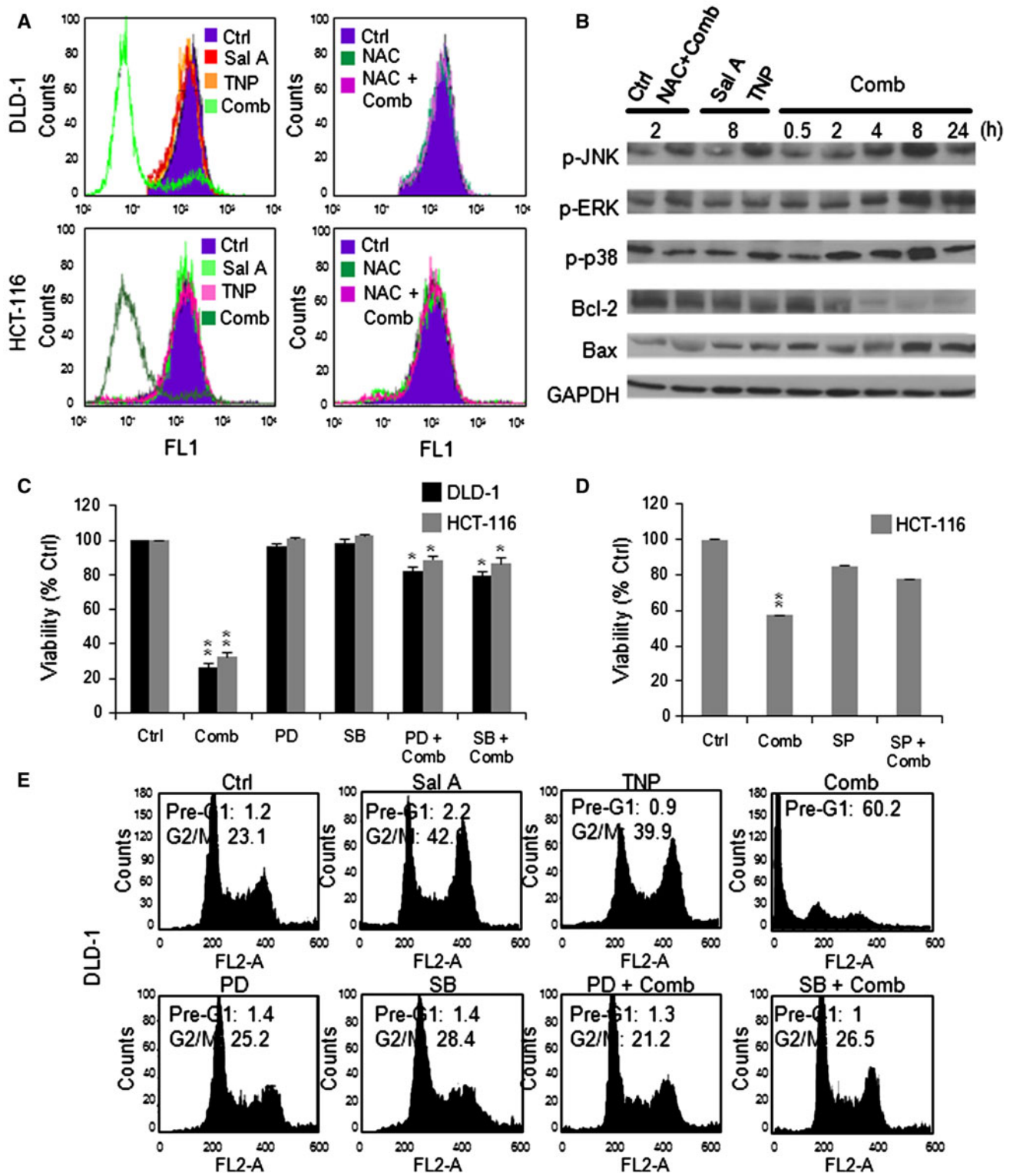
the mitochondrial membrane potential of DLD-1 and HCT-116 cells. However, the combination induced a major disruption of the mitochondrial membrane potential as measured by the reduced accumulation of the fluorescent rhodamine dye. As expected, pre-treatment of the cells with NAC totally reversed the permeabilization of the mitochondrial membrane, which confirms the role of ROS in the induction of cell death. Consistently, the expression level of pro-apoptotic Bax was increased in a time-dependent manner when treated with the combination, while Bcl-2 protein expression was decreased (Fig. 4b), which further confirms the involvement of mitochondria in drug-induced apoptosis [20].

The involvement of the MAPKs pathway in ROS-induced cell death is well established [21]. Consequently, we studied the expression levels of p-ERK (Tyr 204), p-p38 (Tyr 182) and p-JNK (Thr 183, Tyr 185) (Fig. 4b). The protein levels of all tested MAPKs in treated DLD-1 cells increased starting 4 h post-treatment. Densitometry analysis showed that the maximal induction was 2.5-, 2- and 2-fold for p-JNK, p-ERK and p-p38 proteins, respectively, at 8 h after treatment. Interestingly, the increased expression of p-JNK protein in response to the combination treatment appeared to heavily rely on TNP, while the activation of ERK and p38 was observed only when the two compounds were combined (Fig. 4b).

To evaluate whether the activation of the MAPK pathway was implicated in the cell death mechanism induced by the combined drugs, we performed cell viability assays after pre-treatment of cells with 10 μM of the specific ERK inhibitor (PD98059), p38 inhibitor (SB203580) or JNK inhibitor (SP600125) (Fig. 4c, d). The viability in the presence of the specific ERK and p38 inhibitors was reduced by only 15 % (HCT-116) and 20 % (DLD-1), versus an 80 % reduction when Sal A was combined with TNP in the absence of inhibitors (Fig. 4c). The viability of HCT116 was significantly higher when cells were pre-treated with the JNK inhibitor prior to combination treatment (Fig. 4d). These results suggest the involvement of the MAPKs in the antitumor mechanism of the combined drugs. Cell cycle analysis in the presence of the ERK and p38 inhibitors also showed a reversal of the Pre- G_1 accumulation of DLD-1 cells treated with Sal A and TNP (Fig. 4e).

Cell death mechanism is caspase-independent

Caspases are known to be major mediators of apoptosis, mainly through the activation of caspase-8 which triggers the extrinsic apoptosis pathway or through the activation of caspase-9 which triggers the intrinsic pathway [22]. We investigated the involvement of caspase-9 because its activation is stress-induced and mediates the mitochondrial



apoptotic intrinsic pathway. To this aim, we determined the effect of the specific inhibitor of caspase-9 (Z-LEHD-fmk) on cell viability and cell cycle regulation of HCT-116 and DLD-1 cells. Figure 5a indicates that pre-treatment of both

cell lines with 20 μ M of caspase-9 inhibitor did not reverse the inhibition in cell viability induced by the combination treatment, although linalyl acetate and terpeniol combination-induced cell death was reversed by 20 μ M of caspase-

Fig. 4 Cell death mechanism induced by the combination treatment involves mitochondrial membrane permeabilization and MAPKs activation. DLD-1 and HCT-116 cells were treated with Sal A (3 µg/mL for 6 h), TNP (5 µg/mL for 6 h), the combination (3 µg/mL Sal A with 5 µg/mL TNP for 6 h), the antioxidant NAC (5 mM for 2 h), or NAC (5 mM for 2 h) followed by the combination (3 µg/mL Sal A with 5 µg/mL TNP for 6 h). The effect of the different treatments on the mitochondrial membrane potential was assessed using rhodamine assay as described in “Materials and methods” (a). The FL1 signal recorded corresponds to the fluorescent light emitted by the rhodamine dye. The expression levels of the MAPKs proteins p38, ERK and JNK and of the pro-apoptotic Bax and anti-apoptotic Bcl-2 proteins were assessed by Western blotting of DLD-1 cells treated, at the indicated time points, with Sal A (3 µg/mL), TNP (5 µg/mL), their combination (3 µg/mL Sal A with 5 µg/mL TNP) or with 2 h NAC (5 mM) followed by the combination (3 µg/mL Sal A with 5 µg/mL TNP). Representative Western blots from one of two independent experiments (b). DLD-1 and HCT-116 cells were treated with Sal A (3 µg/mL for 24 h), TNP (5 µg/mL for 24 h), the combination (3 µg/mL Sal A with 5 µg/mL TNP for 24 h), the p38 inhibitor PD98058 (PD) (10 µM for 1 h), the ERK inhibitor SB203580 (SB) (10 µM for 1 h), PD (10 µM for 1 h) followed by the combination treatment or SB (10 µM for 1 h) followed by the combination treatment, and the effects of the different treatments on cell viability was assessed (c). HCT116 were treated with the combination (3 µg/mL Sal A with 5 µg/mL TNP for 8 h), the JNK inhibitor SP (SP) (10 µM for 1 h) or SP (10 µM for 1 h) followed by the combination treatment and the effects of the different treatments on cell viability was assessed (d). Each value represents the mean \pm SD of two independent separate experiments each in duplicates. Statistical significance: $**P < 0.01$ comparing combination alone with combination + SP600125 using *t* test. DLD-1 and HCT-116 cells were treated with Sal A (3 µg/mL for 24 h), TNP (5 µg/mL for 24 h), the combination (3 µg/mL Sal A with 5 µg/mL TNP for 24 h), the p38 inhibitor PD98058 (PD) (10 µM for 1 h), the ERK inhibitor SB203580 (SB) (10 µM for 1 h), PD (10 µM for 1 h) followed by the combination treatment or SB (10 µM for 1 h) followed by the combination treatment, and the effects of the different treatments on cell cycle distribution (e) were assessed as described. Representative histograms from one of the two separate experiments are shown; each value represents the mean \pm SD of two independent experiments each in triplicates. Statistical significance: $**P < 0.01$ and $*P < 0.05$ with respect to the control using Dunnett’s multiple comparison test

9 inhibitor in HCT116 cells in a previous study by our group [23]. The same result was obtained with respect to cell cycle progression of DLD-1 cells (Fig. 5b). Furthermore, Western blot analysis showed that, in response to the combination treatment, not only pro-caspase-9 but also its downstream effector pro-caspase-3 were not cleaved (data not shown). Therefore, these experiments rule out the involvement of caspases in apoptosis induced by Sal A and TNP.

Discussion

The most popular anticancer drugs today are plant-derived [4, 24]. SLs are promising anticancer agents known to differentially modulate cancer-related pathways [24]. Here, we show that the two SLs, Sal A and TNP, respectively

isolated from *C. ainetensis* and *A. falcata*, selectively inhibited the viability of several human colon cancer cells but had limited effect on normal cells.

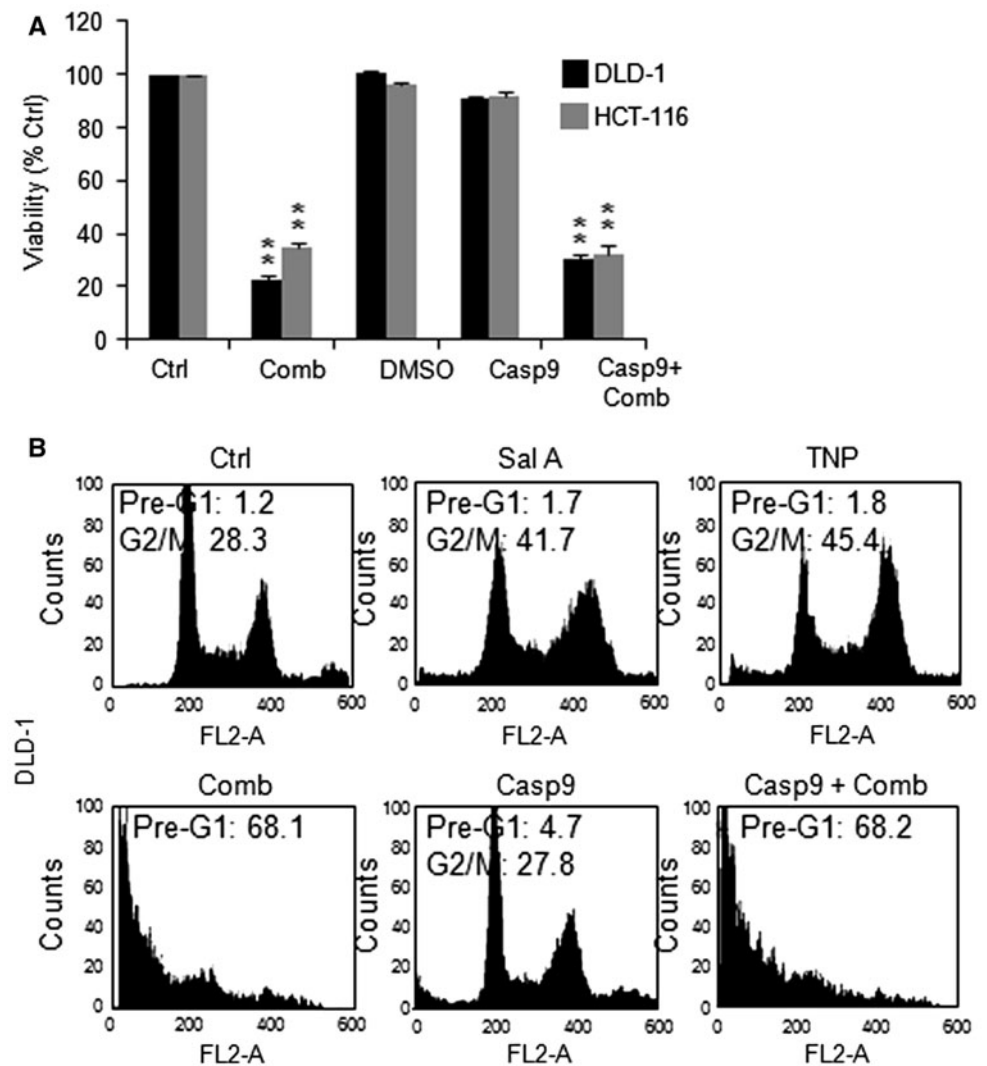
The main advantage of combination treatments is the possibility of limiting the non-specific toxicity that is often observed with high-dosage single-treatment modalities. In the present study, we found that the treatment of cells with low doses of Sal A or TNP alone did not affect cell viability, whereas their combination at the same concentrations synergistically sensitized human colon cancer cell lines and triggered massive cell death by apoptosis. Our results indicating that the cell death caused by the combination treatment is related to their ability to produce ROS are in accordance with previous studies showing that SLs generate high levels of ROS which positively correlate with the degree of cytotoxicity [21].

The anticancer effects of many plant-derived and clinically used chemotherapeutic agents, including parthenolide, are mediated, at least in part, by increasing intracellular ROS levels [16, 25, 26]. Sal A and TNP combination treatment significantly increased ROS and could therefore be an attractive strategy for sensitizing tumor cells to cell death. ROS production may be attributed to the drugs’ ability to directly interact with glutathione and other thiol-bearing enzymes, disrupt the cellular redox balance by depleting the intracellular thiols and induce oxidative stress, leading subsequently to cell death [4, 21, 27].

Apoptosis, the predominant mechanism of cell death triggered by SLs [21], is an effective anticancer mechanism [24, 28]. Consistently, Sal A and TNP in combination triggered cell death by apoptosis. Apoptosis in malignant cells is triggered by either targeting the mitochondrial or the receptor pathways of apoptosis [28–30]. An early event in the mitochondrial apoptotic cascade is the reduction of mitochondrial membrane potential, which may be a sign of mitochondrial swelling and membrane permeabilization [19]. Both Bcl-2 and Bax are apoptosis-related proteins implicated in the apoptotic mitochondrial pathway [20]. We found that the combination of Sal A and TNP induced a collapse in mitochondrial membrane potential and significantly increased the ratio of Bax to Bcl-2 proteins. The accumulation of intracellular ROS accounted for the disruption of the mitochondrial membrane and apoptosis, as supported by the reversal of these effects in the presence of several antioxidants including NAC, which is able to inhibit oxidative stress by scavenging ROS and replenishing glutathione (GSH). Elimination of pro-oxidation by NAC significantly suppressed the cytotoxic effects of Sal A and TNP, indicating that the drug-induced apoptosis may be partially mediated by pro-oxidation.

The MAPKs pathway plays an important role in the transduction of apoptotic signals initiated by toxic stimuli or stress [31, 32]. Currently, there are three known

Fig. 5 Cell death mechanism induced by Sal A and TNP combination treatment is caspase-independent. HCT-116 and DLD-1 cells were treated with the combination (3 μg/mL Sal A with 5 μg/mL TNP for 24 h), control solvent DMSO, caspase-9 inhibitor Z-LEHD-FMK (Casp-9) (applied at 20 μM for 1 h) and caspase-9 inhibitor applied at 20 μM for 1 h prior to the combination treatment (3 μg/mL Sal A with 5 μg/mL TNP for 24 h) and the effects of the different treatments on cell viability (a) and cell cycle changes (b) were determined. In b, representative histograms from one of the three separate experiments are shown; each value represents the mean of three separate experiments each in duplicate. Statistical significance: ***P* < 0.01 with respect to control using Dunnett’s multiple comparison test



MAPKs: the extracellular signal-regulated kinase (ERK1/2), the c-Jun N-terminal kinase/stress-activated protein kinase (JNK), and p38. The activation of ERK, JNK and p38 is a key event in the induction of cell death triggered by SLs [32]. In addition, recent evidence indicates that ROS accumulation results in sustained JNK and p38 activation, leading to cell death [33–35]. Our study demonstrates that the protein expression levels of p-JNK, p-ERK and p-p38 increased in cells treated with the drug combination, reaching its maximum 8 h after treatment. p-JNK expression levels were modulated by TNP and not by Sal A. The alleviation of the combination-mediated antitumor effects in the presence of the ERK and p38 specific inhibitors emphasizes a critical contribution of the MAPKs pathway in Sal A and TNP combination treatment-induced cell death. Interestingly, the SL thapsigargin, which has reached the clinic, causes cell death by specifically activating ERK and p38 in response to ROS [36]. Additionally, the maximal

activation of the MAPKs that was observed at the same time as Bcl-2 reduction suggests a putative involvement of the MAPKs in Bcl-2 inhibition.

The regulation of p-JNK by TNP but not by Sal A highlights the drugs’ ability to differentially target members of the same pathway. Therefore, it would be interesting to determine how TNP affects well-known targets of Sal A in order to elucidate the similarities and differences in the drugs’ mechanisms of action. In fact, three major pathways are reported in SLs’ sensitization of cancer cells to clinical chemotherapeutic agents, namely ROS production, regulation of the MAPK family of proteins and NF-κB inhibition [21]. While none of the drugs generated ROS separately at the concentrations used, TNP differentially modulated the MAPK pathway and Sal A was previously shown to regulate NF-κB [16]. This suggests that Sal A and TNP can be attractive candidates for adjuvant therapy with other clinically used drugs.

Conclusions

In conclusion, our study provides the first evidence that the combination of the two SLs, Sal A and TNP, enhanced apoptosis in human colon cancer cells through ROS production, disruption of mitochondrial membrane potential, activation of ERK, JNK and p38, and upregulation of the Bax/Bcl-2 ratio. The similarity between the mode of action of the Sal A and TNP combination with the clinical SLs parthenolide and thapsigargin suggests that combining Sal A and TNP may be an effective approach for cancer therapy. Future experiments are underway to further understand the mechanism of action of these combined drugs as well as to assess their effects in animal models.

Acknowledgments This work was supported by grants from UNISANTIS and the research was conducted under the direction of the Nature Conservation Center for Sustainable Futures (Ibsar) at the American University of Beirut, Lebanon. We would like to thank members of the Central Research Science Laboratory at the American University of Beirut, Lebanon for their technical assistance with the use of the flow cytometer.

Conflict of interest The authors declare that they have no competing financial interests.

References

- Azaizeh H, Saad B, Cooper E, Said O (2008) Traditional Arabic and Islamic medicine, a reemerging health aid. *Evid Based Complement Alternat Med* 7(4):419–424
- Fakhoury I, Gali-Muhtasib H (2011) Salograviolide A: a plant-derived sesquiterpene lactone with promising anti-inflammatory and anticancer effects. In: Gali-Muhtasib Hala (ed) *Advances in cancer therapy*. InTech Publishing Group, Croatia, pp 369–388
- Kaufman PB, Cseke LJ, Warber S, Duke JA, Briellmann HL (1998) *Natural products from plants*, 1st edn. CRC Press, New York
- Ghantous A, Gali-Muhtasib H, Vuorela H, Saliba N, Darwiche N (2010) What made sesquiterpene lactones reach cancer clinical trials? *Drug Discov Today* 15:668–678
- Berger TG, Dieckmann D, Efferth T, Schultz ES, Funk JO, Baur A, Schuler G (2005) Artesunate in the treatment of metastatic uveal melanoma—first experiences. *Oncol Rep* 14:1599–1603
- Christensen SB, Skytte DM, Denmeade SR, Dionne C, Moller JV, Nissen P, Isaacs JT (2009) A Trojan horse in drug development: targeting of thapsigargin towards prostate cancer cells. *Anticancer Agents Med Chem* 9:276–294
- Efferth T (2007) Willmar Schwabe award 2006: antiplasmodial and antitumor activity of artemisinin—from bench to bedside. *Planta Med* 73:299–309
- Guzman ML, Rossi RM, Neelakantan S, Li X, Corbett CA, Hassane DC, Becker MW, Bennett JM, Sullivan E, Lachowicz JL, Vaughan A, Sweeney CJ, Matthews W, Carroll M, Liesveld JL, Crooks PA, Jordan CT (2007) An orally bioavailable parthenolide analog selectively eradicates acute myelogenous leukemia stem and progenitor cells. *Blood* 110:4427–44359
- Pan MH, Chiou YS, Cheng AC, Bai N, Lo CY, Tan D, Ho CT (2007) Involvement of MAPK, Bcl-2 family, cytochrome c, and caspases in induction of apoptosis by 1,6-O,O-diacetyl-britannilactone in human leukemia cells. *Mol Nutr Food Res* 51:229–238
- Saliba N, Dakdouki S, Homeidan FR, Kogan J, Bouhadir K, Talhouk SN, Talhouk R (2009) Bio-guided identification of an anti-inflammatory guaianolide from *Centaurea ainetensis*. *Pharm Biol* 47:701–707
- Ghantous A, Nasser N, Saab I, Darwiche N, Saliba N (2009) Structure-activity relationship of seco-tanaparholides isolated from *Achillea falcata* for inhibition of HaCaT cell growth. *Eur J Med Chem* 44:3794–3797
- Daniewski WM, Nowak G, Routsis E, Rychlewska U, Szczepanska B, Skibicki P (1992) Salograviolide A, a sesquiterpene from *Centaurea salonitana*. *Phytochemistry* 31:2891–2893
- Vajs V, Todorovic N, Ristic M, Tesovic V, Todorovic B, Janackovic P, Marin P, Milosavljevic S (1999) Guaianolides from *Centaurea nicolai*: antifungal activity. *Phytochemistry* 52:383–386
- Barbour EK, Al Sharif M, Sagherian VK, Habre AN, Talhouk R, Talhouk SN (2004) Screening of selected indigenous plants of Lebanon for antimicrobial activity. *J Ethnopharmacol* 93:1–7
- Al-Saghir J, Al-Ashi R, Salloum R, Saliba N, Talhouk R, Homaidan FR (2009) Anti-inflammatory properties of salograviolide A purified from Lebanese plant *Centaurea ainetensis*. *BMC Complement Altern Med* 9:36
- Ghantous A, Abou Tayyoun A, Abou Lteif G, Saliba N, Gali-Muhtasib H, El-Sabban M, Darwiche N (2008) Purified salograviolide A isolated from *Centaurea ainetensis* causes growth inhibition and apoptosis in neoplastic epidermal cells. *Int J Oncol* 32:841–849
- El-Najjar N, Dakdouki S, Darwiche N, El-Sabban M, Saliba N, Gali-Muhtasib H (2008) Anti-colon cancer effects of salograviolide A isolated from *Centaurea ainetensis*. *Oncol Rep* 19:897–904
- Luna-Herrera J, Costa MC, Gonzalez HG, Rodrigues AI, Castillo PC (2007) Synergistic antimycobacterial activities of sesquiterpene lactones from *Laurus* spp. *JAC* 59:548–552
- Verschoor ML, Wilson LA, Singh G (2010) Mechanisms associated with mitochondrial-generated reactive oxygen species in cancer. *Can J Physiol Pharmacol* 88:204–219
- Cory S, Huang DC, Adams JM (2003) The Bcl-2 family: roles in cell survival and oncogenesis. *Oncogene* 22:8590–8607
- Zhang S, Won YK, Ong CN, Shen HM (2005) Anti-cancer potential of sesquiterpene lactones: bioactivity and molecular mechanisms. *Curr Med Chem Anticancer Agents* 5:239–249
- Fiers W, Beyaert R, Declercq W, Vandenabeele P (1999) More than one way to die: apoptosis necrosis and reactive oxygen damage. *Oncogene* 18:7719–7730
- Itani W, El-Banna SH, Hassan SB, Larsson RL, Bazarbachi A, Gali-Muhtasib H (2008) Anti colon cancer components from Lebanese sage (*Salvia libanotica*) essential oil. *Cancer Biol Ther* 7:1765–1773
- Darwiche N, El-Banna S, Gali-Muhtasib H (2007) Cell cycle modulatory and apoptotic effects of plant-derived anticancer drugs in clinical use or development. *Expert Opin Drug Discov* 2:361–379
- Zhang S, Ong CN, Shen HM (2004) Critical roles of intracellular thiols and calcium in parthenolide-induced apoptosis in human colorectal cancer cells. *Cancer Lett* 208:143–153
- Hadzic T, Aykin-Burns N, Zhu Y, Coleman MC, Leick K, Jacobson GM, Spitz DR (2010) Paclitaxel combined with inhibitors of glucose and hydroperoxide metabolism enhances breast cancer cell killing via H₂O₂-mediated oxidative stress. *Free Radic Biol Med* 48:1024–1033
- Schmidt TJ, LyB G, Pahl HL, Merfortb I (1999) Helenanolide type sesquiterpene lactones, Part 5: the role of glutathione

- addition under physiological conditions. *Bioorg Med Chem* 7:2849–2855
28. Kaufmann SH, Earnshaw WC (2000) Induction of apoptosis by cancer chemotherapy. *Exp Cell Res* 256:42–49
 29. Dirsh VM, Stuppner H, Vollmar AM (2001) Helenalin triggers a CD95 death receptor-independent apoptosis that is not affected by overexpression of Bcl-x(L) or Bcl-2. *Cancer Lett* 61:5817–5823
 30. Lee MG, Lee KT, Chi SG, Park JH (2001) Costunolide induces apoptosis by ROS-mediated mitochondrial permeability transition and cytochrome C release. *Biol Pharm Bull* 24:303–306
 31. Benhar M, Engelberg D, Levitski A (2002) ROS, stress-activated kinases and stress signaling in cancer. *EMBO Rep* 3:420–425
 32. Zhang S, Lin ZN, Yang CF, Shi X, Ong CN, Shen HM (2005) Suppressed NF-kappaB and sustained JNK activation contribute to the sensitization effect of parthenolide to TNF-alpha-induced apoptosis in human cancer cells. *Carcinogenesis* 25:2191–2199
 33. Cho BJ, Im EK, Kwon JH, Lee KH, Shin HJ, Oh J, Kang SM, Chung JH, Jang Y (2005) Berberine inhibits the production of lysophosphatidylcholine-induced reactive oxygen species and the ERK1/2 pathway in vascular smooth muscle cells. *Mol Cells* 20:429–434
 34. Guyton KZ, Liu Y, Gorospe M, Xu Q, Holbrook NJ (1996) Activation of mitogen-activated protein kinase by H₂O₂: role in cell survival following oxidant injury. *J Biol Chem* 271:4138–4142
 35. Kamata H, Honda S, Maeda S, Chang L, Hirata H, Karin M (2005) Reactive oxygen species promote TNF α -induced death and sustained JNK activation by inhibiting MAP kinase phosphatases. *Cell* 120:649–661
 36. Lotem J, Kama R, Sachs L (1999) Suppression or induction of apoptosis by opposing pathways downstream from calcium-activated calcineurin. *Proc Natl Acad Sci USA* 96:12016–12020